Advanced Fiber Materials (2019) 1:126–136
https://doi.org/10.1007/s42765-019-00008-9

RESEARCH ARTICLE

N-Halamine Functionalized Electrospun Poly(Vinyl Alcohol-*co*-Ethylene) Nanofibrous Membranes with Rechargeable Antibacterial Activity for Bioprotective Applications

Mingguang Liang[1] · Fei Wang[2] · Mei Liu[1] · Jianyong Yu[1,2,3] · Yang Si[1,2,3] · Bin Ding[1,2,3]

Received: 29 May 2019 / Accepted: 26 July 2019 / Published online: 19 August 2019

Abstract

Developing bioprotective materials with bactericidal activity is of great significance since it can effectively keep healthcare workers from infection by emerging infectious diseases; however, this is still a big challenge. Herein, we fabricate a novel rechargeable *N*-halamine antibacterial material by functionalizing electrospun poly(vinyl alcohol-*co*-ethylene) (EVOH) nanofibers with dimethylol-5,5-dimethylhydantoin (DMDMH). The premise of the design is that the *N*-halamine compound, DMDMH, can be covalently grafted on the nanofibers, endowing the EVOH nanofibrous membranes (ENM) with rechargeable and durable bactericidal activity. The as-prepared DMDMH functionalized ENM (EDNM) render rechargeable chlorination capacity (> 2000 ppm), high inactivation efficacy against bacteria (> 99.9999% within 3 min), high filtration efficiency (> 99.5%) under low air resistance, and robust mechanical properties, which are due to the synergistic effect of the unique characters of *N*-halamines and electrospun nanofibrous architecture. The successful synthesis of the *N*-halamine antibacterial membranes can serve as a functional layer of protective equipment that capable of inactivating and intercepting pathogenic bioaerosols, providing new ways into the development of new-generation antibacterial bioprotective materials.

Graphic Abstract

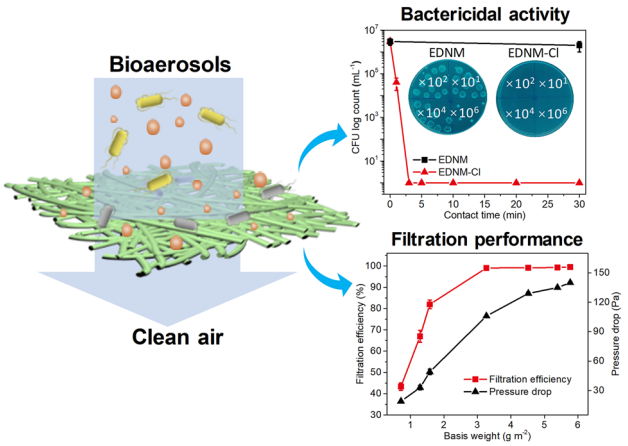

Keywords Electrospinning · Nanofibers · Rechargeable · Antibacterial · Bioprotective applications

Mingguang Liang and Fei Wang contributed equally to the work.

Electronic supplementary material The online version of this article (https://doi.org/10.1007/s42765-019-00008-9) contains supplementary material, which is available to authorized users.

Extended author information available on the last page of the article

Introduction

Emerging infectious diseases (EIDs) have been considered as a major global public health threat [1, 2]. EIDs, such as Middle East respiratory syndrome virus, pandemic H1N1,

and Ebola virus disease, caused incalculable death and afflicted millions of people annually [3]. By way of example, the outbreak of Ebola in West Africa caused nearly 30,000 confirmed patients and over 10,000 deaths, according to the data of the World Health Organization [4]. Particularly, the healthcare workers (HCWs) who were committed to deliver care and services to infected patients suffered from a high risk of acquisition of work-related infectious illnesses [5]. In the epidemic area, the protective equipment for HCWs played a critical role in preventing the transmission of pathogens, involving face shields, protective suits, and gloves [6]. Whereas current protective equipment is typically a temporary physical interception, rather than thoroughly inactivation of pathogens [7]. Accordingly, more effective and durable bioprotective materials to provide antibacterial protection are highly needed, especially for the emergency medical aid outdoors.

Currently, a variety of disinfectants are introduced to design and develop antibacterial materials, such as quaternary ammonium salt, silver nanoparticles, chitosan, and peptides, which can effectively prevent and control bacteria contamination [8–12]. However, these disinfectants experience various problems like irreversible consumption of disinfectants, slow inactivation rate, and poor durability, putting limitations on their practical use in bioprotective applications. Alternatively, *N*-halamine compounds that generated by the halogenation of nitrogen–hydrogen (N–H) bonds-containing precursors hold great promise as antibacterial materials in bioprotection field due to their integrated properties of rechargeable bactericidal activity, rapid inactivation rate, good human and environmental safety, and high durability [13, 14]. In view of their outstanding potential, several researches have been performed via directly using *N*-halamine precursor polymers that contained N–H bonds (such as polyamide and aramid) to develop *N*-halamine antibacterial materials, but the strong hydrogen bonds between the polymer chains inhibit the conversion of N–H groups to bactericidal *N*-halamine groups and the type of these polymers is limited [15, 16]. Besides, a few explorative works suggested that *N*-halamine antibacterial materials could be constructed by physically coating or blending *N*-halamine compound into substrate [17–19]; however, these compounds might be wiped off from the substrate when an external force was applied on the material, resulting in a dramatic decrease of the bactericidal activity. Therefore, it is still a challenge to fabricate covalently incorporated and structurally stable *N*-halamine materials with rechargeable antibacterial activity.

In addition to the powerful and rechargeable bactericidal activity, air filtration performance is of equal importance to the bioprotective materials, which can effectively decontaminate bioaerosols that containing pathogenic particles [20, 21]. More recently, benefiting from the high specific surface area, small pore size, tunable tortuous open-porous structures, and high porosity, electrospun nanofibrous materials showed great potential to construct bioprotective materials with excellent filtration performance [22–25]. Taking electrospun nanofibrous membranes as the substrate and further coupling with *N*-halamine bactericidal groups has been considered as a promising approach to fabricate bioprotective materials with rechargeable antibacterial and excellent filtration performance.

Herein, we demonstrate an effective and facile strategy to create rechargeable antibacterial nanofibrous membranes by grafting dimethylol-5,5-dimethylhydantoin (DMDMH) onto poly(vinyl alcohol-*co*-ethylene) (EVOH) nanofibers. As far as we know, this is the first time that electrospun EVOH nanofibrous membranes (ENM) is functionalized with DMDMH to fabricate bactericidal membranes for bioprotective applications. The *N*-halamine precursor compound, DMDMH, is covalently grafted on EVOH nanofibers, ensuring the durable and rechargeable bactericidal activity of the membranes. The resulting DMDMH functionalized ENM (EDNM) exhibited the integrated properties of rechargeable chlorination capacity, excellent bactericidal activity, high particle removal efficacy, and robust breathability, which can serve as a scalable bactericidal and filtration layer of bioprotective equipment.

Experimental Section

Materials

EVOH (ethylene content of 27 mol%) was obtained from Kuraray Co., Ltd., Japan. Aqueous solutions of DMDMH (solid content of 55 wt%) were purchased from Shanghai Wanhou Biotechnology Co., Ltd., China. Isopropyl alcohol (IPA), magnesium chloride ($MgCl_2$), hydrochloric acid (HCl), and sodium hydroxide (NaOH) were bought from Aladdin Chemistry Co., Ltd., China. A bleach solution with 3.4 wt% to 4.6 wt% of active chlorine content was supplied by Jiangsu aitefu group Co., Ltd., China. Iodine (I_2) standardized solution (0.01 N), sodium thiosulfate ($Na_2S_2O_3$) standard solution (0.1 N) were obtained from Acros Organics Co., Ltd., USA. Luriz-Bertani (LB) broth, LB agar and phosphate buffered saline (PBS) buffer were purchased from Shanghai Sangon Biotech Co., Ltd., China.

Preparation of ENM

An 8 wt% EVOH transparent solution was prepared by dissolving 3.2 g of the polymer in a 36.8 g of IPA/deionized water mixture (7/3, v/v) with stirring for 6 h in a water bath at 80 °C. Then the EVOH transparent solution was transferred into the syringes for the following spinning

experiment, and the ENM were fabricated by an electrospinning setup, which was bought from SOF nanotechnology Co., China. The spinning process was operated with a voltage of 30 kV, a fixed speed of 4 mL h^{-1}, and a tip-to-collector distance of 23 cm. The spinning environment temperature was 22 ± 3 °C and the humidity was 50 ± 5%.

Fabrication of EDNM

The EDNM were prepared by first dipping the ENM in an aqueous solution containing DMDMH and the catalyst ($MgCl_2$ at 10% of the weight of DMDMH) for 30 min. Subsequently, the membranes were transferred into a drying oven for 1 h at 50 °C, and then the grafting reaction was carried out for 1 h at 140 °C. The modified membranes from various DMDMH concentration of 0.5, 1, and 3 wt% were named EDNM-0.5, EDNM-1, and EDNM-3, respectively.

Chlorination and Analytical Titration

The bleach solution was diluted to obtain the chlorination solution with active chlorine content of 500 ppm, and then HCl and NaOH were used to adjust the pH value of the solution. Subsequently, the modified membranes were immersed into the chlorination solution for various chlorination time. Then the samples were taken away from the solution and washed thoroughly by deionized water to remove the unbonded free chlorine and DMDMH, followed by drying at 45 °C for 1 h. Active chlorine content of the samples was determined by iodometric titration method. Generally, the sample of 50 mg was put into a beaker containing 15 mL of 0.001 N $Na_2S_2O_3$ standard solution. After stirring for 10 min, the excess amount of $Na_2S_2O_3$ was titrated with 0.001 N I_2 solution. The active chlorine content (ppm) of these chlorinated EDNM (EDNM-Cl) was tested according to iodometric titration method and computed by using the following equation:

$$\frac{35.45 \times (V0 - Ve)}{2m}$$

where V_0 and V_e are the volumes (mL) of the I_2 solution used in titration with EDNM and chlorinated EDNM, respectively, and m is the mass (g) of the sample.

Bacterial Culture and Antibacterial Testing

The *E. coli* (Gram-negative bacteria, ATCC 25922) were incubated in LB broth of 10 mL for 24 h at 37 °C, and then they were harvested and washed twice with PBS by centrifugation. Subsequently, the obtained bacteria were resuspended in diluted LB broth with chemical oxygen demand (COD) of 2000 or sterilized deionized water to get bacterial suspensions with concentration of 3×10^8 CFU mL^{-1} for the following experiments. For the antibacterial testing, the membranes were cut into a circle of 2×2 cm^2 and put in a perforated plate, then each sample was subjected to 10 μL of the bacterial suspensions and incubated on an automated shaker at 37 °C with different contact time. At predetermined time points, a sample loaded with bacteria was taken out and immersed in a test tube that containing sterilized deionized water of 1 mL to obtain the bacterial suspension. Then the suspension was diluted serially ($\times 10^1, \times 10^2, \times 10^4$, and $\times 10^6$) and cultured on agar plates for enumeration.

Morphology Observation of Bacteria

The bacteria were first harvested from the membranes by vortexing and fixed with PBS solution that contained 2.5 wt% of glutaraldehyde for 1 h. Subsequently, the bacteria were dehydrated with a series of ethanol/water solution of 50%, 70%, and 90%. Finally, the bacterial suspension was dropped on fibrous membranes for SEM analysis.

Characterization

The morphologies of the modified nanofibrous membranes and bacteria were investigated using scanning electron microscopy (SEM) (Tescan Vega 3, Czech). The chemical structures of the membranes before and after modification were performed by Fourier transform infrared (FT-IR) spectrometer (Thermo Scientific Nicolet iS10, USA). The dynamic water permeation process on the membranes was recorded by contact angle measurement (Kino SL200B, USA), and a droplet of 5 μL was used. The pore size distribution of the membranes was investigated by the capillary flow porometer (Porous Materials Inc. CFP-1100AI, USA). The tensile property of the samples was measured by using tensile tester (XQ-1C, China). The Brunauer–Emmett–Teller (BET) surface areas and N_2 adsorption–desorption isotherms were investigated by physisorption analyzer (Micromeritics, ASAP 2020, USA). The chemical element composition of the membranes was tested through X-ray photoelectron spectroscopy (XPS) (Escalab 250Xi, USA). The filtration efficiency and pressure drop were characterized using a filter tester (Huada LZC-H, China).

Results and Discussion

Synthesis and Bactericidal Functions of EDNM

We designed the EDNM based on the following three principals: (1) the *N*-halamine moieties should be covalently bonded to nanofibrous membranes, (2) the membranes should be able to inactivate the bacteria and the bactericidal activity is rechargeable, and (3) the pathogenic

particles must be effectively intercepted by the membranes. The first requirement can be satisfied by the grafting reaction between the EVOH nanofiber substrates and the *N*-halamine compound. To meet the other two requirements—the construction of rechargeable bactericidal nanofibrous filter—we combined the unique properties of *N*-halamine compound and electrospun nanofibrous architecture.

Figure 1 displayed the synthesis and bactericidal function of the EDNM-Cl. In view of the excellent water insolubility and abundant active hydroxyl groups [26], EVOH was selected and electrospun into nanofibrous membranes to serve as the substrate of the bactericidal materials. Meanwhile, a bifunctional *N*-halamine precursor, DMDMH, was used as the grafting agent and bactericidal component of the membranes. The DMDMH could form both crosslinking between hydroxyl groups of EVOH nanofibers and grafting on EVOH nanofibers, and the reactive end between two carbonyl groups could be hydrolyzed into N–H group [27]. For *N*-halamine precursor compounds, the N–H groups could become bactericidal nitrogen–chlorine (N–Cl) groups after chlorination. The successful grafting reaction retained the active N–H groups in EDNM, thereby bactericidal N–Cl bonds could be readily formed by exposure to chlorination solution. When the chlorinated membranes contacted with bacteria, the oxidative chlorine released by N–Cl groups would transfer to bacterial cell membranes, and then destroyed them by halogenating amino groups or oxidizing thiol groups in proteins of bacteria, while the N–Cl groups reverted to N–H groups [13, 28]. Interestingly, the active chlorine could be renewable by immersing the EDNM in the chlorination solution again.

Morphologies and Structure of EDNM

The bactericidal properties of the membranes highly depend on the loading amount of the DMDMH and the resulting nanofibrous architecture. Figure 2a–d displayed SEM images of the pristine ENM and EDNM modified from solutions with different concentrations of DMDMH. It was clear that the pristine ENM exhibited a three-dimensional nonwoven geometry consisting of randomly oriented smooth nanofibers. After being modified with DMDMH, a DMDMH layer was grafted on the surface of the EVOH nanofibers. As the increasing concentration of DMDMH, more adhesive structures appeared along with the increasing average nanofiber diameter from 480 to 1035 nm (Figure S1), ascribing to the grafting reaction of DMDMH onto nanofibers. Furthermore, as shown in Fig. 2e, the effective grafting of DMDMH was further confirmed by the analysis of FT-IR spectra. The EDNM exhibited new characteristic peaks around 1139 and 1718 cm^{-1}, which were corresponded to the C–O–C and C=O, respectively, indicating that DMDMH was successfully grafted on EVOH nanofibers [27, 29]. In addition, the water wetting ability of the membranes was significantly improved due to the introduction of the hydrophilic hydantoin groups (Fig. 2f). It could be found that EDNM showed faster water permeation of 3 min than that of the ENM (30 min), which would make good contact with chlorination solutions for the following chlorination treatment.

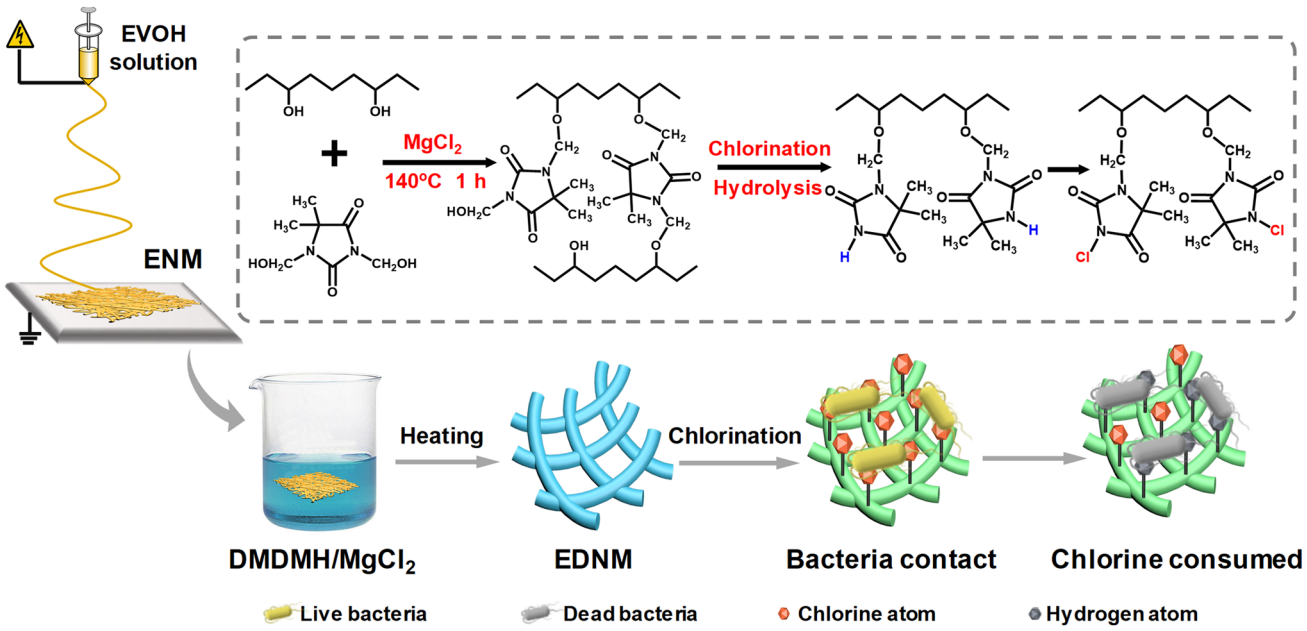

Fig. 1 Illustration showing the design, fabrication, and bactericidal function of as-prepared EDNM-Cl

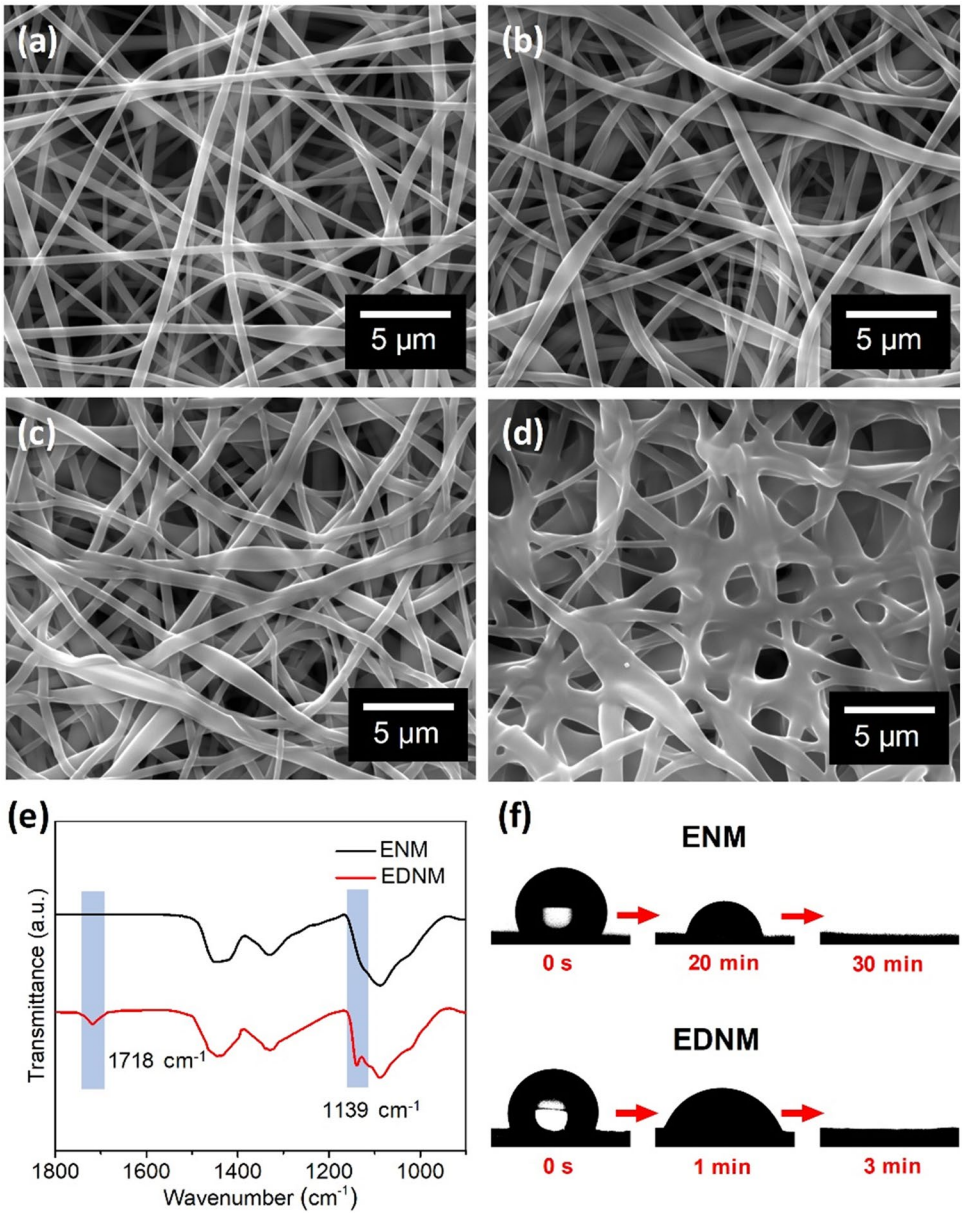

Fig. 2 SEM images of **a** ENM and EDNM with various concentrations of DMDMH: **b** 0.5, **c** 1, and **d** 3 wt%. **e** FT-IR spectra of the ENM and EDNM. **f** Digital images showing the dynamic process of water infiltration on the ENM and EDNM

We further illustrated the pore structures and mechanical properties of EDNM. As we can see from Fig. 3a, the average pore sizes of ENM, EDNM-0.5, EDNM-1, and EDNM-3 were 2.45, 1.40, 1.32, and 1.12 μm, indicating an obvious decrease trend as the concentration of modification solution increased, which was attributed to the formation of the bonding structure among fibers. Mechanical properties of the materials are indispensable in practical use, Fig. 3b exhibited the mechanical properties of the membranes before and after modification. With the increase of the concentration of DMDMH from 0 to 3 wt%, the tensile stress of the membranes increased from 3.1 to 7.3 MPa; meanwhile, the breaking elongation of these membranes reduced from 90 to 71%. This phenomenon was ascribed to the increasing adhesive structure of membranes. On one hand, the increasing adhesive points could enhance the tensile stress when an external force was applied on the nanofibers; on the other hand, they would limit the slippage among fibers during the tensile testing, resulting in the decline of the breaking elongation [30].

To reveal the effect of the modification on the pore structure of the membranes, N_2 adsorption–desorption measurements at 77 K were employed to study the porous structure of the membranes. As shown in Fig. 3c, the N_2 adsorption–desorption isotherm curves represented typical IV type with tiny H3 hysteresis loops, implying the characteristics of mesopores within the ENM and EDNM [31, 32]. The inset of Fig. 3c demonstrated the BET surface areas of the membranes, which revealed slight decrease of the relevant surface area with the increasing DMDMH contents. This

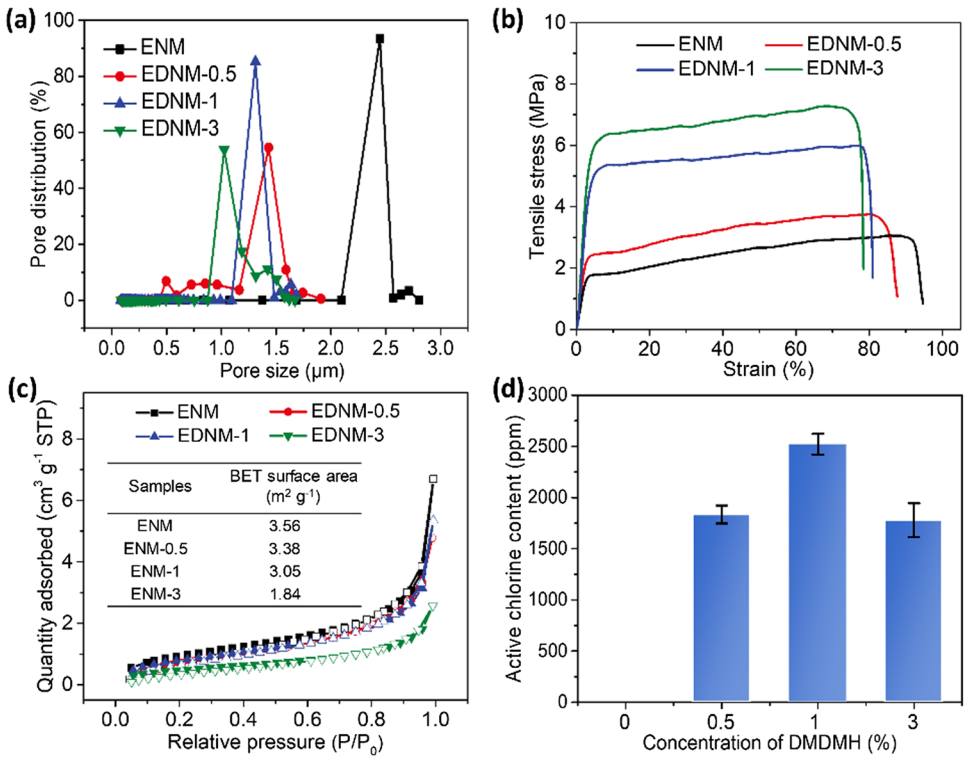

Fig. 3 **a** Pore size distribution and **b** mechanical properties of pristine ENM, EDNM-0.5, EDNM-1, and EDNM-3. **c** N_2 adsorption–desorption isotherms, BET surface area, and **d** active chlorine content of ENM modified with various concentrations of DMDMH

phenomenon illustrated the fact that the DMDMH played a critical role in deciding the surface area of the EDNM, which was ascribed to the increasing fiber diameter as a consequence of the adhesive structure. The membranes were further immersed into the chlorination solution, and then we utilized the iodometric titration method to determine the active chlorine content of the membranes. As we can see from Fig. 3d, the pristine ENM without DMDMH did not loaded with active chlorine due to the lack of N–H groups in EVOH polymer chains. The use of the DMDMH concentrations from 0.5 to 1 wt% presented a dramatic increase in active chlorine contents from 1830 to 2520 ppm, which was attributed to the increased N-Cl groups derived from more available N–H bonds. However, further increasing the concentration of DMDMH (3 wt%) resulted in a decline of active chlorine content. This phenomenon was ascribed to the decreased surface area that reduced the active sites of the nanofibers, revealing that the modification concentration of 1 wt% was enough to endow the EDNM with considerable chlorine content.

Rechargeable Chlorination Capability of EDNM-Cl

In consideration of the active chlorine content of *N*-halamine plays an important role in bactericidal property, we further studied the influence of chlorination time and pH on chlorination ability of the EDNM. As exhibited in Fig. 4a, the active chlorine content increased quickly in the inception phase and reached a stable stage at the chlorination time of 30 min with the saturation value of 2520 ppm. Notably, the traditional *N*-halamine fabrics only achieved active chlorine content of less than 500 ppm, which was one order lower than that of the as-prepared EDNM-Cl [33, 34]. To provide a deep understanding into the chlorination process, chlorination capability at various pH values (1, 3, 5, 7, 9, and 11) was investigated to illustrate the influence of the chlorination pH value on active chlorine content of EDNM-Cl (Fig. 4b). The highest value was achieved at pH of 5, while the active chlorine content was less than 1000 ppm when the samples were chlorinated in strong acidic or alkaline solutions. This resulted from the fact that the highest reaction rate was presented between HClO and N–H groups [35, 36]. When the pH value of chlorination solution ranged from 5 to 6, HClO was the main chlorine species (ClO^-, HClO, Cl_2, etc.) [37], thereby facilitating the reaction of HClO and N–H groups, rendering high active chlorine content of the EDNM-Cl.

In order to understand the chemical composition changes of the membranes before and after chlorination, we analyzed the chemical composition of EDNM and EDNM-Cl by means of XPS (Fig. 4c). Compared with the EDNM, the chlorinated membranes represented a new characteristic peak (Cl 2p at 200.75 eV), indicating that the chlorine had been loaded on the membranes successfully [38, 39]. Additionally, Cl 2p core level spectrum was presented in Figure S2, which was on behalf of the N-Cl bonds. Owing to the renewable feature of *N*-halamine structure, the EDNM-Cl

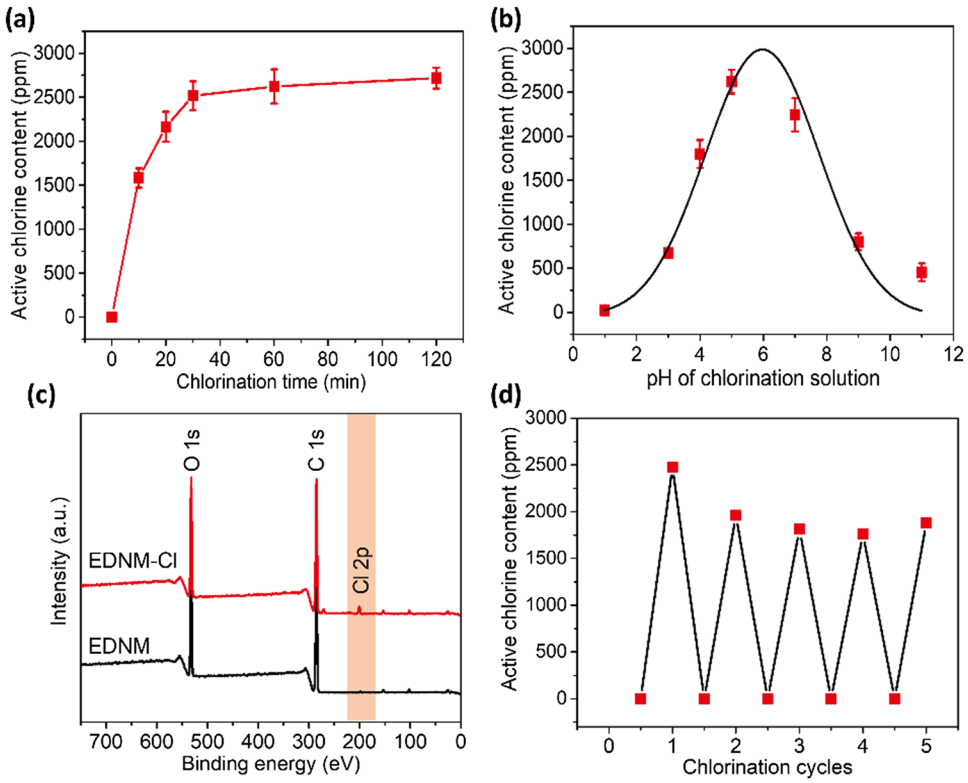

Fig. 4 **a** Active chlorine content of the EDNM-Cl with various chlorination time. **b** The influence of pH on the active chlorine content of THE EDNM-Cl. **c** The XPS survey of THE EDNM-Cl. **d** Cyclic chlorination properties of EDNM-Cl

exhibited rechargeable chlorination capacity. As shown in Fig. 4d, the cyclic chlorination testing of EDNM-Cl was performed, the samples were chlorinated at pH of 5 for 1 h and then impregnated into an excess of $Na_2S_2O_3$ solution to consume all active chlorine. After that, the membranes were washed several times with deionized water and immersed into chlorination solution for the next cycle. Interestingly, the active chlorine content displayed a slight decrease at the second cycle, and then it tended to be stable around 2000 ppm in the following cycles. The robust rechargeable chlorination capability was due to the stability of the *N*-halamine moieties. In addition, the SEM image of the membranes after 5 cycling chlorination tests was investigated. As we can see from Figure S3, there was no significant change in the morphology of the nanofibers after the cycling tests, suggesting the good stability of the nanofibrous architecture.

Bactericidal Activity and Filtration Performance of EDNM-Cl

The EDNM-Cl rendered the integrated properties of high active chlorine content, robust mechanical property, rechargeable *N*-halamine structure, and three-dimensional porous fibrous networks, which made them show great prospects to be promising antibacterial and filtration materials for bioprotective applications. The Gram-negative bacteria, *E. coli* (ATCC 25922), were chosen as the representative bacteria to assess the bactericidal activity of the membranes. For the bactericidal activity assays, about 2 mg of EDNM and EDNM-Cl were loaded with 10 µL of 3×10^8 CFU mL^{-1} bacterial suspensions in deionized water or nutritive broth solution with COD of 2000. After contacting a certain time, the bacteria were harvested and resuspended into bactericidal suspensions, and diluted to be cultured on agar for calculating bacterial colonies by plate count method. Figure 5a illustrated the bactericidal activity of the membranes against *E. coli* with COD of 0. The bacteria grew freely on the plate of control EDNM, whereas no bacteria were seen on the plate of the chlorinated membranes, indicating effective killing against *E. coli* of EDNM-Cl. The chlorinated membranes could inactivate 6 log CFU of *E. coli* within a short contact time of 3 min, which was correspond to a promising inactivation efficacy of 99.9999%. Remarkably, when the COD was 2000, the EDNM-Cl still achieved the ultrahigh bactericidal efficacy within 5 min contact (Fig. 5b). Figure 5c displayed the SEM images of bacteria on EDNM and EDNM-Cl. The bacteria were viable and presented intact bacterial cell structure with typical rod like morphology after contacting with the control EDNM; however, the *E. coli* cells lost their membrane integrity after exposure to EDNM-Cl since the oxidative chlorine released from the chlorinated samples could destroy the cell membranes [40, 41].

To further evaluate the practical utilization of EDNM-Cl for bioprotective applications, we demonstrated the filtration performance of the membranes. Figure 5d exhibited

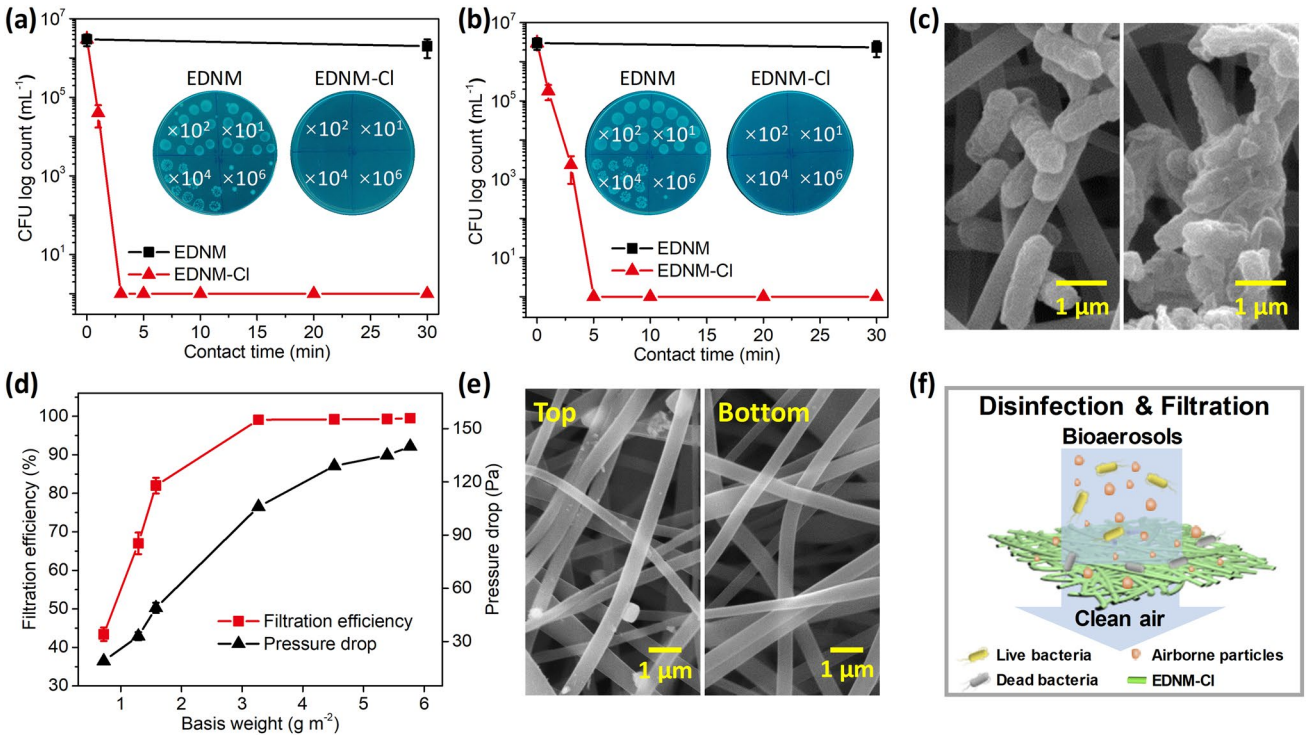

Fig. 5 Bactericidal activity of EDNM and EDNM-Cl against *E. coli* under the conditions with COD of **a** 0 and **b** 2000. **c** SEM images of bacteria on EDNM (left) and EDNM-Cl (right). **d** Filtration efficiency and pressure drop of antibacterial EDNM-Cl. **e** SEM images of the top and bottom surface of EDNM-Cl after filtration. **f** Schematic showing the procedure of disinfection and filtration of EDNM-Cl

the filtration efficiency and pressure drop of EDNM-Cl with virous basis weight, which were determined through feeding a given mass of aerosol containing sodium chloride particles with a diameter of around 0.3–0.5 μm under the flow of 32 L min^{-1}. By increasing the basis weight of EDNM-Cl, the filtration efficiency exhibited distinct increase from 43.4 to 99.5% and the pressure drop showed an increased trend, revealing the critical role of the basis weight in enhancing the filtration performance of membranes [42]. It was clearly visible that the filtration efficiency of EDNM-Cl could reach 99.1% with a low pressure drop of 105 Pa when the basis weight exceeded 3.2 g m^{-2}, which was significantly higher than that of the N95 surgical masks (95%) used by healthcare workers. In addition, the SEM images of the top and bottom surface of EDNM-Cl after filtration were investigated. As we can see from Fig. 5e, almost all particles were trapped on the surface of the membranes, whereas no particle was observed on the bottom of EDNM-Cl, indicating a typical surface filtration for membrane filter media [43]. Based on the above results, we believed that the EDNM-Cl was capable of resisting the invasion of bioaerosols that containing pathogenic bacteria and particles for HCWs, which was similar to the contaminated air in the epidemic area (Fig. 5f). When the bioaerosols passed through the materials, the fine particles and bacteria would be intercepted and inactivated by the nanofibers, yielding the clean air. Most importantly, as shown in Figure S4, a large-scale EDNM-Cl (60×70 cm^2) was readily available, which made it possible for industrial application in bioprotective equipment.

Conclusions

In summary, we developed a novel, effective, and facile strategy for fabricating rechargeable antibacterial *N*-halamine nanofibrous membranes by combining the electrospun ENM and surface functionalization with DMDMH. The rechargeable *N*-halamine moieties were successfully grafted onto nanofibers, endowing the ENM with rechargeable high active chlorine content (> 2000 ppm). Benefiting from the three-dimensional nanofibrous architectures, rechargeable chlorination capacity, ease of industrialization, and robust mechanical properties, the resulting modified membranes exhibited 6 log reduction against typical pathogenic *E. coli* within 3 min of contact time; meanwhile, the membranes rendered high particle removal efficiency (99.1%) and low pressure drops (105 Pa) with the basis weight of 3.2 g m^{-2}. These intriguing attributes enabled the EDNM-Cl to act as a functional layer of the protective equipment, which could intercept and inactivate

the pathogenic air. The successful synthesis of the EDNM-Cl might also open new ways for the development of antibacterial materials for various applications.

Acknowledgements This work was supported by the National Natural Science Foundation of China (Nos. 51773033, and 51673037), and the Shanghai Committee of Science and Technology (No. 18511109500).

Compliance with Ethical Standards

Conflict of interest There are no conflicts to declare.

References

1. Halliday JEB, Hampson K, Hanley N, Lembo T, Sharp JP, Haydon DT, Cleaveland S. Driving improvements in emerging disease surveillance through locally relevant capacity strengthening. *Science*. **2017**;*357*:146.
2. Halloran ME, Longini IM. Emerging, evolving, and established infectious diseases and interventions. *Science*. **2014**;*345*:1292.
3. Metcalf CJE, Lessler J. Opportunities and challenges in modeling emerging infectious diseases. *Science*. **2017**;*357*:149.
4. Ebola Situation Report, W. H. O. Ebola virus disease outbreak http://apps.who.int/ebola/current-situation/ebola-situation-report-30-march-2016.
5. Clever LH, Leguyader Y. Infectious risks for health care workers. *Annu Rev Public Health*. **1995**;*16*:141.
6. Gralton J, McLaws ML. Protecting healthcare workers from pandemic influenza: N95 or surgical masks? *Crit Care Med*. **2010**;*38*:657.
7. Si Y, Zhang Z, Wu WR, Fu QX, Huang K, Nitin N, Ding B, Sun G. Daylight-driven rechargeable antibacterial and antiviral nanofibrous membranes for bioprotective applications. *Sci Adv*. **2018**;*4*:eaar5931.
8. Buffet-Bataillon S, Tattevin P, Bonnaure-Mallet M, Jolivet-Gougeon A. Emergence of resistance to antibacterial agents: the role of quaternary ammonium compounds-a critical review. *Int J Antimicrob Agents*. **2012**;*39*:381.
9. Wu MC, Ma BH, Pan TZ, Chen SS, Sun JQ. Silver-nanoparticle-colored cotton fabrics with tunable colors and durable antibacterial and self-healing superhydrophobic properties. *Adv Funct Mater*. **2016**;*26*:569.
10. Han H, Zhu J, Wu DQ, Li FX, Wang XL, Yu JY, Qin XH. Inherent guanidine nanogels with durable antibacterial and bacterially antiadhesive properties. *Adv Funct Mater*. **2019**;*29*:1806594.
11. Verlee A, Mincke S, Stevens CV. Recent developments in antibacterial and antifungal chitosan and its derivatives. *Carbohydr Polym.* **2017**;*164*:268.
12. Guilhelmelli F, Vilela N, Albuquerque P, Derengowski LD, Silva-Pereira I, Kyaw CM. Antibiotic development challenges: the various mechanisms of action of antimicrobial peptides and of bacterial resistance. *Front Microbiol*. **2013**;*4*:353.
13. Dong A, Wang YJ, Gao Y, Gao T, Gao G. Chemical insights into antibacterial *N*-halamines. *Chem Rev*. **2017**;*117*:4806.
14. Hui F, Debiemme-Chouvy C. Antimicrobial *N*-halamine polymers and coatings: a review of their synthesis, characterization, and applications. *Biomacromolecules*. **2013**;*14*:585.
15. Lee J, Broughton RM, Worley SD, Huang TS. Antimicrobial polymeric materials; cellulose and m-aramid composite fibers. *J Eng Fibers Fabr.* **2007**;*2*:25.
16. Sun YY, Sun G. Novel refreshable *N*-halamine polymeric biocides: *N*-chlorination of aromatic polyamides. *Ind Eng Chem Res*. **2004**;*43*:5015.
17. Bai R, Kang J, Simalou O, Liu WX, Ren H, Gao TY, Gao YY, Chen WJ, Dong A, Jia R. Novel N-Br bond-containing *N*-halamine nanofibers with antibacterial activities. *ACS Biomater Sci Eng*. **2018**;*4*:2193.
18. Bai R, Zhang Q, Li LL, Li P, Wang YJ, Simalou O, Zhang YL, Gao G, Dong A. *N*-halamine-containing electrospun fibers kill bacteria via a contact/release co-determined antibacterial pathway. *ACS Appl Mater Interfaces*. **2016**;*8*:31530.
19. Chen Y, He QK, Ren GY, Feng CY, Li N, Yu H, Han QX. Preparation of biocidal 4-ethyl-4-(hydroxymethyl)oxazolidin-2-one-based *N*-halamine polysiloxane for impregnation of polypropylene in supercritical CO_2. *J Appl Polym Sci*. **2018**;*135*:46624.
20. Demir B, Cerkez I, Worley SD, Broughton RM, Huang TS. *N*-halamine-modified antimicrobial polypropylene nonwoven fabrics for use against airborne bacteria. *ACS Appl Mater Interfaces*. **2015**;*7*:1752.
21. Ren T, Dormitorio TV, Qiao MY, Huang TS, Weese J. *N*-halamine incorporated antimicrobial nonwoven fabrics for use against avian influenza virus. *Vet Microbiol*. **2018**;*218*:78.
22. Si Y, Yu JY, Tang XM, Ge JL, Ding B. Ultralight nanofibre-assembled cellular aerogels with superelasticity and multifunctionality. *Nat Commun*. **2014**;*5*:5802.
23. Zhu ZG, Wang W, Qi DP, Luo YF, Liu YR, Xu Y, Cui FY, Wang C, Chen XD. Calcinable polymer membrane with revivability for efficient oily-water remediation. *Adv Mater*. **2018**;*30*:e1801870.
24. Deuber F, Mousavi S, Federer L, Hofer M, Adlhart C. Exploration of ultralight nanofiber aerogels as particle filters: capacity and efficiency. *ACS Appl Mater Interfaces*. **2018**;*10*:9069.
25. Marriam I, Wang XP, Tebyetekerwa M, Chen GY, Zabihi F, Pionteck J, Peng SJ, Ramakrishna S, Yang SY, Zhu MF. A bottom-up approach to design wearable and stretchable smart fibers with organic vapor sensing behaviors and energy storage properties. *J Mater Chem A*. **2018**;*6*:13633.
26. Fu QX, Wang XQ, Si Y, Liu LF, Yu JY, Ding B. Scalable fabrication of electrospun nanofibrous membranes functionalized with citric acid for high-performance protein adsorption. *ACS Appl Mater Interfaces*. **2016**;*8*:11819.
27. Sun G, Xu XJ, Bickett JR, Williams JF. Durable and regenerable antibacterial finishing of fabrics with a new hydantoin derivative. *Ind Eng Chem Res*. **2001**;*40*:1016.
28. Kaur R, Liu S. Antibacterial surface design—contact kill. *Prog Surf Sci*. **2016**;*91*:136.
29. Babar AA, Miao DY, Ali N, Zhao J, Wang XF, Yu JY, Ding B. Breathable and colorful cellulose acetate-based nanofibrous membranes for directional moisture transport. *ACS Appl Mater Interfaces*. **2018**;*10*:22866.
30. Zhao J, Li Y, Sheng JL, Wang XF, Liu LF, Yu JY, Ding B. Environmentally friendly and breathable fluorinated polyurethane fibrous membranes exhibiting robust waterproof performance. *ACS Appl Mater Interfaces*. **2017**;*9*:29302.
31. Ge JL, Wang F, Yin X, Yu JY, Ding B. Polybenzoxazine-functionalized melamine sponges with enhanced selective capillarity for efficient oil spill cleanup. *ACS Appl Mater Interfaces*. **2018**;*10*:40274.
32. Ge JL, Zhang JC, Wang F, Li ZL, Yu JY, Ding B. Superhydrophilic and underwater superoleophobic nanofibrous membrane with hierarchical structured skin for effective oil-in-water emulsion separation. *J Mater Chem A*. **2017**;*5*:497.
33. Liu Y, Liu Y, Ren XH, Huang TS. Antimicrobial cotton containing *N*-halamine and quaternary ammonium groups by grafting copolymerization. *Appl Surf Sci*. **2014**;*296*:231.
34. Ma KK, Xie ZW, Jiang QY, Li J, Li R, Ren XH, Huang TS, Zhang KQ. Cytocompatible and regenerable antimicrobial

cellulose modified by *N*-halamine triazine ring. *J Appl Polym Sci*. **2014**;*131*:46027.
35. Si Y, Li JY, Zhao CY, Deng Y, Ma Y, Wang D, Sun G. Biocidal and rechargeable *N*-halamine nanofibrous membranes for highly efficient water disinfection. *ACS Biomater Sci Eng*. **2017**;*3*:854.
36. Pastoriza C, Antelo JM, Amoedo FA, Parajó M. Kinetic study of the formation reaction of *N*-chloro-2-oxazolidinone. *J Phys Org Chem*. **2015**;*28*:602.
37. Deborde M, von Gunten U. Reactions of chlorine with inorganic and organic compounds during water treatment-kinetics and mechanisms: a critical review. *Water Res*. **2008**;*42*:13.
38. Liu C, Shan HR, Chen XX, Si Y, Yin X, Yu JY, Ding B. Novel inorganic-based *N*-halamine nanofibrous membranes as highly effective antibacterial agent for water disinfection. *ACS Appl Mater Interfaces*. **2018**;*10*:44209.
39. Liu Y, Li J, Cheng XL, Ren XH, Huang TS. Self-assembled antibacterial coating by *N*-halamine polyelectrolytes on a cellulose substrate. *J Mater Chem B*. **2015**;*3*:1446.
40. Fang G, Li WF, Shen XM, Perez-Aguilar JM, Chong Y, Gao XF, Chai ZF, Chen CY, Ge CC, Zhou RH. Differential Pd-nanocrystal facets demonstrate distinct antibacterial activity against gram-positive and gram-negative bacteria. *Nat Commun*. **2018**;*9*:129.
41. Tao Y, Ju EG, Ren JS, Qu XG. Bifunctionalized mesoporous silica-supported gold nanoparticles: intrinsic oxidase and peroxidase catalytic activities for antibacterial applications. *Adv Mater*. **2015**;*27*:1097.
42. Hua T, Li YY, Zhao XL, Yin X, Yu JY, Ding B. Stable low resistance air filter under high humidity endowed by self-emission far-infrared for effective $PM_{2.5}$ capture. *Compos Commun*. **2017**;*6*:29.
43. Cui HM, Li YY, Zhao XL, Yin X, Yu JY, Ding B. Multilevel porous structured polyvinylidene fluoride/polyurethane fibrous membranes for ultrahigh waterproof and breathable application. *Compos Commun*. **2017**;*6*:63.

Mingguang Liang received his B.S. degree from Qingdao University of Science & Technology, China, in 2017. He is currently a master student in the College of Materials Science and Engineering in Donghua University. His research mainly focuses on the electrospun nanofibrous membranes and bioprotective materials.

Fei Wang received her B.S. degree from Wuhan Textile University, China, in 2014. She is now a Ph.D. candidate in the College of Textiles in Donghua University. Her current research interests include the fabrication and application of antibacterial nanofibrous membranes/aerogel materials.

Mei Liu received her B.S. degree from Huaibei Normal University, China, in 2017. She is currently a master student in the College of Materials Science and Engineering in Donghua University. Her current research interests mainly focus on the antibacterial nanofibrous membranes and food packaging materials.

Dr. Jianyong Yu received his B.S., M.S., and Ph.D. degrees in College of Textiles in Donghua University in 1985, 1988 and 1991, respectively. He is currently a full professor in Innovation Center for Textile Science and Technology in Donghua University and an academician of Chinese Academy of Engineering. His research interests include natural and synthetic fibers, functional textile materials, textile composites, and industrial textiles.

Dr. Yang Si received his B.S. from Sichuan University, China, in 2009. After that he earned his Ph.D. degree from Donghua University, China, in 2015. Currently, he is a full professor in Innovation Center for Textile Science and Technology in Donghua University. His research mainly focuses on antibacterial bioprotective materials, water disinfection materials, and nanofibrous aerogels.

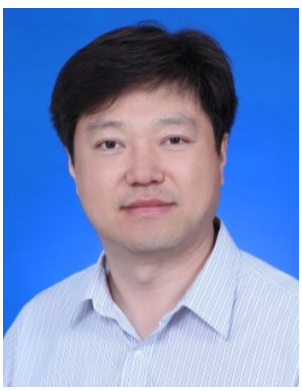

Dr. Bin Ding received his B.S. from Northeast Normal University, China, in 1998, and his M.S. from Chonbuk National University, Korea, in 2003. Afterward, he earned his Ph.D. degree from Keio University, Japan, in 2005. He is now a full professor in Innovation Center for Textile Science and Technology in Donghua University. His research mainly focuses on filtration materials, waterproof and breathable fabrics, oil-water separation materials, flexible ceramic nanofibers, and nanofiber aerogels.

Affiliations

Mingguang Liang[1] · Fei Wang[2] · Mei Liu[1] · Jianyong Yu[1,2,3] · Yang Si[1,2,3] · Bin Ding[1,2,3]

✉ Yang Si
yangsi@dhu.edu.cn

✉ Bin Ding
binding@dhu.edu.cn

[1] State Key Laboratory for Modification of Chemical Fibers and Polymer Materials, College of Materials Science and Engineering, Donghua University, Shanghai 201620, China

[2] College of Textiles, Donghua University, Shanghai 201620, China

[3] Innovation Center for Textile Science and Technology, Donghua University, Shanghai 200051, China